IEEE Access
Multidisciplinary | Rapid Review | Open Access Journal

Received October 15, 2020, accepted November 2, 2020, date of publication November 5, 2020, date of current version November 20, 2020.

Digital Object Identifier 10.1109/ACCESS.2020.3036033

Equivalent Consumption Minimization Strategy With Consideration of Battery Aging for Parallel Hybrid Electric Vehicles

BIN ZHOU[1], (Member, IEEE), JEFFREY B. BURL[1], (Senior Member, IEEE), AND AMIR REZAEI[2]

[1]Department of Electrical and Computer Engineering, Michigan Technological University, Houghton, MI 49931, USA
[2]Systems Engineering Department, Pi Innovo LLC, Plymouth, MI 48170, USA

Corresponding author: Bin Zhou (binz@mtu.edu)

ABSTRACT The equivalent consumption minimization strategy (ECMS) is a well-known energy management strategy for Hybrid Electric Vehicles (HEV). ECMS is very computationally efficient since it yields an instantaneous optimal control. ECMS has been shown to minimize fuel consumption under certain conditions. But, minimizing the fuel consumption often leads to excessive battery damage. This paper introduces a new optimal control problem where the cost function includes terms for both fuel consumption and battery aging. The Ah-throughput method is used to quantify battery aging. ECMS (with the appropriate equivalence factor) is shown to also minimize the cost function that incorporates battery aging. Simulation results show that the proposed aging ECMS algorithm significantly improves battery aging with little or no fuel economy penalty compared to ordinary ECMS.

INDEX TERMS Battery aging, hybrid electric vehicle, energy management strategies, optimal control, equivalent consumption minimization strategy.

I. INTRODUCTION

The Hybrid Electric Vehicles (HEVs), considered in this paper, have two energy sources: combustible fuel and an electric battery. The Energy Management (EM) strategy determines how much of each source are used to satisfy the drivers demands. The EM strategy impacts both fuel economy [1] and battery aging [2]. The battery is an expensive component of the HEV. Therefore, more and more studies of EM in HEV applications have been considering improving the battery aging [3]–[9].

Some well-studied energy management strategies for HEVs are rule-based control (RBC) [10], the equivalent consumption minimization strategy (ECMS) [11], [12], model predictive control [13], and dynamic programming [14]. RBC is computationally fast. Also, the design and implementation of RBC is intuitive for the expert designer. However, improving performance of a RBC requires large amounts of calibration work. Some studies have shown that the performance of RBC is poor in comparison with strategies like ECMS or model predictive control [15]. Model predictive control yields close to the optimal fuel economy [16], [17]. However, MPC requires prediction of the power that will be demanded by the driver in the future. Since many statistical factors affect the driver's behavior, accurate estimation of the future demanded power is challenging [18]. Dynamic programming yields the optimal fuel economy. However again, implementation of dynamic programming also requires knowledge of the future demanded power, and is intractable for real-time applications [14].

ECMS is an instantaneous (greedy) optimization algorithm. The ECMS cost function includes fuel usage and also applies a penalty for using battery power. The weighting for this penalty is known as the equivalence factor. ECMS can be derived using Pontryagin's Minimum principle (PMP) [19]. Thus, ECMS yields optimal fuel economy provided the battery state of charge does not reach the limits [11]–[13]. But, determining the optimal equivalence factor requires knowledge of the entire drive-cycle, a priori. This knowledge is not typically available. For practical applications, adaptive ECMS (A-ECMS) is proposed that estimates the optimal ECMS equivalence factor [20]. A-ECMS also is used to maintain the battery state of

The associate editor coordinating the review of this manuscript and approving it for publication was Xiaosong Hu.

charge within the constraints. In A-ECMS, the equivalence factor is calculated either with an instantaneous estimation algorithm [21] or using a prediction-based estimation [22].

The general ECMS cost function only considers the total energy drawn from both fuel tank and the battery. Thus, even though optimal controllers will improve the fuel economy, these controllers may perform poorly with regard to battery life. To meet the driver's demanded power, the control strategy may charge or discharge the battery quickly and frequently. This behavior has an undesirable effect on battery life.

As stated in [23], [24], a high rate or depth of discharge or charge will shorten battery life. The Ah-throughput battery aging method presented in [26], is introduced, modified, and modeled in this work. The Ah-throughput battery aging model is semi-empirical. This model is also known as a performance model. Compared to direct measurement [27], equivalent circuit model [28], electrochemical model [29], analytical model [30], and statistical method [31], the performance model yields better life prediction [32]. Since the inputs used for EM are continuously measured or estimated, the Ah-throughput method can also be used for real-time monitoring.

The Ah-throughput method used in this work has been modified compare to [2], [3], [7], [26]. The nominal values of C-rate and state of charge (SOC) identified in [2], [3], [26], [36] are constants. But, these constants depend on the driving conditions or drive cycle used to develop the empirical model. Therefore, the results are not independent of drive-cycle. Further, the calculation for severity factor is drive-cycle or driving behavior dependent as well as the normalized Ah-throughput. Note that the normalized Ah-throughput will be used in the battery aging term of the cost function which directly influences the optimal power split. In this paper, these values have been modified to be the average values over a combination of drive cycles. In addition, a heat-generation model has been added to estimate the battery pack temperature.

As mentioned in [3], the battery size, described by the available battery energy capacity, will affect the energy management of the HEV. In our previous papers [44], [45], we also observed that the change of battery capacity due to state of charge constraints or environment temperature changes significantly influence ECMS performance. Therefore, the ratio between battery pack energy capacity and fuel contained energy is considered when developing the cost function.

Our previous work in [11] introduced upper and lower bounds on the equivalence factor λ^*, which are independent of drive cycle and depend only on the average efficiency values of the powertrain components. This work will show that ECMS is still optimal if a battery aging term is added to the Hamiltonian. In addition, the bounds on the equivalence factor are shown to still be applicable with the battery aging term included. Lastly, it is verified that battery aging is improved significantly by using the new Aging ECMS algorithm.

The main contribution of this work is considered as: the proposed formula of ECMS Hamiltonian equation with battery aging consideration which is drive-cycle independent; and the proof of equivalence factor bounds in the aging ECMS, which could be used for future adaptive ECMS equivalence factor control law.

This work is organized as follows: The plug-in HEV vehicle model and the general ECMS EM strategy are introduced in Section II. In Section III, the battery aging model is presented; the Aging ECMS problem formulation is introduced, and the ECMS optimal control is presented. Simulation results are shown in Section IV; and conclusions are in Section V.

II. GENERAL ECMS EQUIVALENCE FACTOR BOUNDS

A. VEHICLE MODEL

Fig.1 shows the vehicle configuration used in this work. This typical configuration of Parallel HEV coupled engine and e-motor by a coupling belt then connected to the transmission input shaft. Therefore, the vehicle could be operated in engine only mode, battery only mode and hybrid mode.

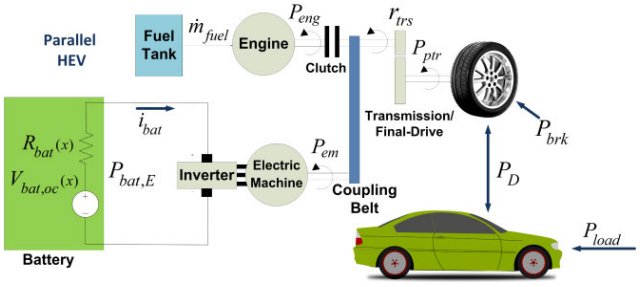

FIGURE 1. Typical configuration of a Parallel HEV.

The driver uses the acceleration pedal or brake pedal to control the driver's demanded power P_D to achieve the desired speed. Therefore, the hard constraint of the EM strategy is set to meet P_D at any given time t

$$P_D = P_{ptr}(t) + P_{brk}(t) \tag{1}$$

where P_{ptr} is the powertrain power provided by the internal combustion engine and/or the electric motor/generator in watts. P_{brk} is the power provided by the friction brake system (W).

Assuming both the belt and the clutch, shown in Fig.1, have no loss, then eq. (1) can be written:

$$\begin{cases} Brake, Coast P_D \le 0 : P_{brk}(t) = P_D(t) - \dfrac{P_{em}(t)}{\eta_{trs}(r_{trs}(t))} \\ Accelerate, Cruise P_D > 0 : P_{eng}(t) = \dfrac{P_D(t)}{\eta_{trs}(r_{trs}(t))} - P_{em}(t) \end{cases} \tag{2}$$

where P_{em} is the net output power of the electric machine and P_{eng} is the net output power of the engine in watts.

η_{trs} is the total efficiency of the transmission which depends on the gear ratio r_{trs}. Since P_D is known in (2), the electric motor power and the efficiencies, specify the engine power. Therefore, only the net electric machine power and the gear ratio are included in the control vector:

$$u(t) = [r_{trs}(t)\, P_{em}(t)]^T \tag{3}$$

B. GENERAL ECMS

The optimal control that minimizes the fuel consumption is:

$$u^* = \underset{u}{argmin} \left\{ \int_0^{tf} \dot{m}_{fuel}(x, u)dt \right\} \tag{4}$$

where $\dot{m}_f$ is the fuel mass flow rate (gram/s), t_f is the time at the end of drive-cycle, u is the vector of control actions, u^* is the vector of optimal control actions, and x is the state variable. The control problem is subject to the following constraints:

$$u \in U \tag{5}$$
$$P_D(t) = P_{ptr}(t) + P_{brk}(t) \tag{6}$$
$$\dot{x} = -\frac{P_{bat,C}(x(t), u(t))}{Q_{bat} V_{bat,oc}(x(t))} \tag{7}$$
$$SOC_L \le x \le SOC_H \tag{8}$$

Eq. (5) specifies that the control satisfies all constraints, where U is the space of the admissible control actions that do not violate any power or speed limit on any powertrain components, like engine speed/torque limits, battery limits, etc. Constraint (6) guarantees that driver's demanded power will be satisfied by u, and thus, the reference vehicle speed will be tracked closely by the energy management strategy. x is the battery SOC and (7) is the state equation of the system, where $P_{bat,C}$ is the total chemical power output from the battery in Watts; Q_{bat} is the battery capacity in Ah and $V_{bat,oc}$ is the battery pack open-circuit voltage in Volts. Eq (8) specifies that the battery SOC is constrained to be between a high SOC limit and low SOC limit.

The Hamiltonian for the optimal control problem specified above is:

$$\begin{aligned} H &= \dot{m}_{fuel}(\boldsymbol{u}(t), P_D(t)) + p(t)\,\dot{x}(x(t), u(t)) \\ &= \dot{m}_{fuel}(\boldsymbol{u}(t), P_D(t)) - p(t)\,\frac{P_{bat,C}(x(t), u(t))}{Q_{bat} V_{bat,oc}(x(t))} \end{aligned} \tag{9}$$

where Eq. (7) is used to substitute for $\dot{x}(x(t), u(t))$ to yield the second expression. Since $\dot{m}_{fuel}$ is independent of the state $x(t)$ and when constraints (8) are satisfied, $V_{bat,oc}$ and $P_{bat,C}(x(t), u(t))$ are nearly independent of $x(t)$. Therefore, the derivative of the Hamiltonian equation is approximately equal to zero.

$$\dot{p}^*(t) = -\frac{\partial H}{\partial x} \approx 0 \Rightarrow p^* \textit{is a constant} \tag{10}$$

Defining $\lambda = -p/(Q_{bat} V_{bat,oc}(x))$, the Hamiltonian, becomes the ECMS cost function:

$$H = \dot{m}_{fuel}(\boldsymbol{u}(t), P_D(t)) + \lambda P_{bat,C}(x(t), u(t)) \tag{11}$$

where λ is the ECMS equivalence factor.

In our previous work [11], we have shown that λ^* (the superscript $*$ denotes the optimal value) for a parallel HEV lies within the range:

$$\frac{1}{Q_{lhv}} \le \lambda^* \le \frac{\bar{\eta}_{em}\bar{\eta}_{inv}\bar{\eta}_{bat}}{Q_{lhv}\bar{\eta}_{eng}} \tag{12}$$

where Q_{lhv} is the fuel lower heating value, and $\bar{\eta}_{em}$, $\bar{\eta}_{inv}$, $\bar{\eta}_{bat}$, and $\bar{\eta}_{eng}$ are the average efficiency values of the e-machine, inverter, battery, and engine respectively.

III. AGING ECMS

A. BATTERY AGING MODEL

Battery SOC is calculated as the integral of battery current I_{batt} [26] plus the initial value of SOC_0.

$$SOC(t) = SOC_0 - \frac{1}{Q_{bat}} \int_0^t I_{batt}(\tau)\, d\tau \tag{13}$$

Battery capacity loss Q_{loss}, in percentage, is [26], [32]:

$$Q_{loss} = B * \exp\left(-\frac{E_a}{RT_{cell}}\right) (Ah)^z \tag{14}$$

Equation (14) is derived using the semi-empirical method. E_a is the total activation energy in J·mol^{-1}, R is the universal gas constant, T_{cell} is the battery cell temperature in Kelvin, Ah is the total Ah-throughput in Ah, and z is the power-law factor.

The power-law factor z is found by curve-fitting of Eq. (15):

$$ln(Q_{loss}) = ln(B) - \frac{E_a}{RT} + z ln(Ah) \tag{15}$$

See Wang [23]. Per Wang's experimental data, z has a constant value of 0.56 for temperatures 15, 45 and 60°C. The environmental temperature used in this work is $20 = 293.15$ in K.

In equation (14), B is called the pre-exponential factor and it is a function of SOC. The coefficient B is computed via curve fitting from experimental data using the equation:

$$B = \alpha \cdot SOC + \beta \tag{16}$$

where α and β are identified using experimental data. E_a is a function of I_c, the C-rate, as follows:

$$E_a = -31700 + 163.3 \cdot I_c \tag{17}$$

where I_c in hr^{-1} is given by:

$$I_c = \frac{|I_{batt}|}{Q_{batt}} \tag{18}$$

Now, the percentage of capacity loss is found by substituting (16) and (17) into (14):

$$Q_{loss\%} = (\alpha \cdot SOC + \beta) \cdot exp\left(\frac{-31700 + 163.3 \cdot I_c}{R \cdot T_{cell}}\right) \cdot Ah^z \tag{19}$$

Maxime's state space model in [33] estimates the battery cell temperature from the air temperature, battery current and battery internal resistance. This state space temperature

estimation model uses heat transfer and equivalent resistance modeling. The state space model provided in [24] is:

$$\begin{cases} \dot{T}_{cell} = k_1 \left(R_{batt} I_{batt}^2 - k_4 \left(T_{cell} - T_{sens} \right) \right) \\ \dot{T}_{sens} = k_2 \left(k_4 \left(T_{cell} - T_{sens} \right) - k_5 \left(T_{sens} - T_{cas} \right) \right) \\ \dot{T}_{cas} = k_3 \left(k_5 \left(T_{sens} - T_{cas} \right) - k_6 \left(T_{cas} - T_{air} \right) \right) \end{cases} \quad (20)$$

where T_{air} is the external environment air temperature, T_{cas} is the casing temperature outside of the battery pack, T_{sens} is the sensor temperature inside the battery pack, and T_{cell} is the temperature on the surface of the battery cell. An assumption was made in this battery model that the heat generated by the cell has been equally distributed inside the battery pack. The parameters in (20) are calculated by:

$$\begin{cases} k_1 = \dfrac{1}{C_{v1}} \quad k_2 = \dfrac{1}{C_{v2}} \quad k_3 = \dfrac{1}{C_{p3}} \\ k_4 = \dfrac{1}{R_{eff\,1}} \quad k_5 = \dfrac{1}{R_{eff\,2}} \quad k_6 = \dfrac{1}{R_{eff\,3}} \end{cases} \quad (21)$$

where C_{v1} is the heat capacity at constant volume J/K of the cell; C_{v2} is the heat capacity of the air trapped inside the battery pack; C_{p3} is the heat capacity of the external air. $R_{eff\,1}$ is the thermal resistance between the inside of the battery pack and the outside of the battery cell (calculated by the area swept by the cooling air and the heat transfer coefficient); $R_{eff\,2}$ is the thermal resistance between the outside of the battery pack and the inside of the battery pack; $R_{eff\,3}$ is the thermal resistance between the external environment and the outside of the battery pack.

From [2], [26], the total Ah-throughput computed from the nominal current I_{nom}, is defined as the total charge contained in the battery during its entire life:

$$\Gamma = \int_0^{EOL} |I_{nom}(t)|\, dt \quad (22)$$

The severity factor is defined as the ratio of the nominal theoretical total Ah-throughput to the actual total Ah-throughput [35], [36], which contains the aging effects of different operating load cycles. The severity factor will be greater than one if the battery is carrying a more severe load, otherwise, less than one [26]. Shorter battery life is expected when the severity factor is greater than one.

$$\sigma\left(I_c, T_{cell}, SOC\right) = \frac{\Gamma}{\gamma(I, \theta, SOC)} = \frac{\int_0^{EOL} |I_{nom}(t)|\, dt}{\int_0^{EOL} |I(t)|\, dt} \quad (23)$$

A capacity loss of 20% from the original battery capacity is considered the end of life. The equation below (for nominal total Ah-throughput) is calculated by setting $Q_{loss}\%$ equal to 20%, to find the value of Ah. The nominal total Ah-throughput Γ is then:

$$\Gamma = \left[\frac{20}{(\alpha \cdot SOC_{nom} + \beta) \cdot exp\left(\frac{-31700 + 163.3 \cdot I_{c,nom}}{R \cdot T_{cell}} \right)} \right]^{\frac{1}{z}} \quad (24)$$

where SOC_{nom}, and $I_{c,nom}$ are the nominal values of SOC and I_c. The nominal values have been calculated based on the average of the historical values. This throughput is defined in terms of a nominal SOC and average C-rate. The actual total Ah-throughput are calculated by the instantaneous SOC and C-rate.

$$\gamma = \left[\frac{20}{(\alpha \cdot SOC(t) + \beta) \cdot exp\left(\frac{-31700 + 163.3 \cdot I_c(t)}{R \cdot T_{cell}} \right)} \right]^{\frac{1}{z}} \quad (25)$$

The effective total Ah-throughput can be calculated by integrating the severity factor times the absolute value of the battery current [26], [35], [36].

$$Ah_{eff}(t) = \int_0^t \sigma(I_c, T_{cell}, SOC) \cdot |I(\tau)| d\tau \quad (26)$$

The effective Ah-throughput gives the battery life cost for each drive cycle in Ampere-hours. The absolute value of current, used in (26), indicates that there is an implicit assumption that charging and discharging have the same impact on battery aging. The battery is considered at its end of life when Ah_{eff} reaches the value of Γ [2], [3], [26]. Thus, the battery State of Health (SOH) is calculated as:

$$SOH = \left(1 - \frac{Ah_{eff}}{\Gamma} \right) \cdot 100\% \quad (27)$$

A SOH equal to zero indicates that the battery capacity loss has reached 20% and the battery is at its end of life. The initial SOH for each drive cycle is assumed to be 100% in this paper.

B. AGING ECMS

The optimal control that minimizes the total fuel consumption with consideration of battery aging degradation is written as:

$$u^* = \underset{u}{argmin} \left\{ \int_0^{tf} \dot{m}_{fuel}(x, u) + k \cdot \dot{Ah}_{eff}(\sigma, I_{bat}) dt \right\} \quad (28)$$

where k is the aging coefficient yields a compromise between fuel consumption and battery aging. And again, $\dot{m}_f$ is the fuel mass flow rate in gram/s, $\dot{Ah}_{eff}$ is the rate of effective Ah-throughput, x is the state variable defined as state of charge, u is the vector of control actions, u^* is the optimized control action, σ is the severity factor defined in equation (23), and I_{bat} is the battery cell current. The control problem is subject to following the constraints defined in equation or inequalities (5)(6)(7)(8). Which guarantees that all constraints will not be violated by the control action u, driver's demanded power will be satisfied by u, the state equation of the system is defined and within the limited bounds.

According to [14], the fundamental lemma of the calculus of variations, the Hamiltonian equation can be optimized by solving the costate variable, which will minimize the cost function defined in equation (28).

$$H = \dot{m}_{fuel}(u(t), P_D(t)) + k \cdot \dot{Ah}_{eff}(x(t), u(t)) + p(t) \cdot \dot{x}(x(t), u(t)) \quad (29)$$

The derivative of effective Ah-throughput is obtained from Eq. (26):

$$\dot{Ah}_{eff}(t) = \sigma(I_c(t), T_{cell}(t), x(t)) \cdot |I_{bat}(t)| \quad (30)$$

Substituting equation (7) and (30) into equation (29) yields the Hamiltonian:

$$H = \dot{m}_{fuel}\left(u\left(t\right), P_D\left(t\right)\right) + k \cdot \sigma\left(I_c\left(t\right), T_{cell}\left(t\right), x(t)\right) \cdot \left|I_{bat}\left(t\right)\right| - p\left(t\right) \cdot \frac{P_{bat,C}\left(x\left(t\right), u\left(t\right)\right)}{Q_{bat} V_{bat,oc}\left(x\left(t\right)\right)} \quad (31)$$

where $p\left(t\right)$ is the co-state, and it is defined as:

$$\dot{p}\left(t\right) = -\frac{\partial H}{\partial x} = -k \cdot \frac{\partial \sigma\left(I_c\left(t\right), T_{cell}\left(t\right), x\left(t\right)\right)}{\partial x} \cdot \left|I_{bat}\left(t\right)\right| - k \cdot \sigma\left(I_c\left(t\right), T_{cell}\left(t\right), x\left(t\right)\right) \frac{\partial}{\partial x}\left|I_{bat}\left(t\right)\right| + p\left(t\right) \cdot \frac{\partial}{\partial x} \frac{P_{bat,C}\left(x\left(t\right), u\left(t\right)\right)}{Q_{bat} \cdot V_{bat,oc}\left(x\left(t\right)\right)} \quad (32)$$

$V_{bat,oc}$ is almost constant in charge-sustaining mode [41]–[43] within the SOC constraints defined in equation (8), therefore, the last 2 terms in equation (32) are independent of state variable x

$$\begin{cases} \dfrac{\partial}{\partial x}\left|I_{bat}\left(t\right)\right| = \dfrac{\partial}{\partial x} \dfrac{P_{bat,C}\left(x\left(t\right), u\left(t\right)\right)}{V_{bat,oc}\left(x\left(t\right)\right)} = 0 \\ \dfrac{\partial}{\partial x} \dfrac{P_{bat,C}\left(x\left(t\right), u\left(t\right)\right)}{Q_{bat} \cdot V_{bat,oc}\left(x\left(t\right)\right)} = 0 \end{cases}$$

Therefore,

$$\dot{p}\left(t\right) = -k \cdot \frac{\partial \sigma\left(I_c\left(t\right), T_{cell}\left(t\right), x\left(t\right)\right)}{\partial x} \cdot \left|I_{bat}\left(t\right)\right| \quad (33)$$

According to [35], [36], the derivative of the severity factor with respect to SOC is approximately zero within the *SOC* constraints defined in (8), thus

$$\dot{p}\left(t\right) = -\frac{\partial H}{\partial x} \approx 0 \Rightarrow p^* \textit{ is constant} \quad (34)$$

Hence, a constant value for the costate p still yields the global optimal solution, as long as the constraints defined in (8) are met.

Defining $\lambda = -p/(Q_{bat} V_{bat,oc}(x))$, the Hamiltonian equation can be written as the ECMS cost function with an additional term that penalizes battery aging:

$$H = \dot{m}_{fuel}\left(u\left(t\right), P_D\left(t\right)\right) + k \cdot \dot{Ah}_{eff}\left(x\left(t\right), u\left(t\right)\right) + \lambda \cdot P_{bat,C}\left(x\left(t\right), u\left(t\right)\right) \quad (35)$$

From (34), the optimal value of λ is a constant [11], [12].

C. AGING COEFFICIENT K

The battery capacity affects the performance of the optimal EMS as discussed in our previous papers [44], [45]. The energy capacity ratio, defined

$$k_R = R_{Energy,Cap} = \frac{E_{useful,bat}}{E_{useful,fuel}} = \frac{E_{bat,cap} * \eta_{bat}}{E_{fuel,cap} * \eta_{eng}} \quad (36)$$

represents the relative energy contribution of the battery and the fuel. Less battery capacity results in a smaller hybridization ratio of the HEV, i. e., a smaller relative energy contribution of the battery compared to the fuel. This results in battery fading having a smaller effect on performance. Also, a smaller battery pack is less expensive compared to the entire vehicle. Therefore, it is expected that k should scale with the energy capacity ratio. Simulations presented later in the paper will bear out this assumption.

The optimal control is obtained by minimizing the Hamiltonian in Eq. (35) at every point in time [14]. Therefore, we need to minimize a linear combination of the power used and the fading power of the battery. The power used includes both the power in the fuel and the power out of the battery. Insight into the relative contribution of these terms can be obtained by rewriting the optimal control problem in terms of energy (and including the energy out of the battery):

$$u^* = \underset{u}{argmin}\left\{a \cdot E_{bat,f} + E_{loss}\right\} \quad (37)$$

where $E_{Bat,f}$ is the equivalent battery energy capacity lost due to battery fading, E_{loss} is the total powertrain lost energy during the trip, and $a = a_0 \cdot k_R$ is proportional to k. Note that a is used here because the change of variables in the cost function results in a different value. But, a is still a weighting factor that provides a tradeoff between battery fading and powertrain efficiency. Note that a is a constant in this work, but could be adaptively adjusted due to battery capacity variation (fading) and temperature change in future work.

The powertrain lost energy is:

$$E_{loss} = E_{fuel} + E_{bat,C} - E_D \quad (38)$$

where E_{fuel} is the energy contained in the fuel consumed, $E_{bat,C}$ is the battery chemical energy consumed, and E_D is the driver demanded energy. So, the optimal control problem can be given as:

$$u^* = \underset{u}{argmin}\left\{a \cdot E_{bat,f} + E_{fuel} + E_{bat,C} - E_D\right\} \quad (39)$$

Energy is the integral of power, so

$$u^* = argmin\left\{\int_0^{t_f} \left(P_{fuel} + P_{bat,C} + a \cdot \dot{Ah}_{eff} \cdot V_{ocv} \cdot 3600 - P_D\right) dt\right\} \quad (40)$$

where P_D is the demanded power which is not controllable. Therefore:

$$\begin{aligned} u^* &= argmin\left\{\int \left(P_{fuel} + P_{bat,C} + a \cdot \dot{Ah}_{eff} \cdot V_{bat,oc} \cdot 3600\right) dt\right\} \\ &= argmin\left\{\int \left(\dot{m}_{fuel} \cdot Q_{lhv} + P_{bat,C} + a \cdot V_{bat,oc} \cdot 3600 \cdot \dot{Ah}_{eff}\right) dt\right\} \end{aligned} \quad (41)$$

Defining:

$$k_0 = \frac{3600 \cdot V_{bat,oc}}{Q_{lhv}} \quad (42)$$

$$k = a_0 \cdot k_R \cdot k_0 \quad (43)$$

where k_0 is for unit conversion. Therefore:

$$u^* = argmin\left\{\int\left(\dot{m}_{fuel} + \frac{1}{Q_{lhv}}P_{bat,C} + k\cdot\dot{Ah}_{eff}\right)dt\right\} \quad (44)$$

The values of k with different battery capacities are shown in Table 1.

TABLE 1. Value of *k* in different battery pack size Honda CIVIC IMA 13.2 gallons fuel tank.

Battery Capacity	Value of k
1 kWh battery pack	0.0064
2 kWh battery pack	0.0129
4 kWh battery pack	0.0258

D. BOUNDS OF THE AGING ECMS EQUIVALENCE FACTOR

Finding the optimal equivalence factor, in general, requires solution of a two-point boundary value problem which requires that the driver's demanded power for the whole drive be available at the start of the drive. But, comparing Eq. (44) and (35) we see that $\lambda = 1/Q_{lhv}$. Also, we expect that fuel usage is minimized by maximizing the use of the battery when ignoring the state of charge constraints. Therefore, we expect that $\lambda = 1/Q_{lhv}$ will maximize the use of the electric motors. This behavior is confirmed by the simulations which show that this equivalence factor results in the battery SOC quickly reaching the lower bound SOC_L. A smaller λ makes the battery energy even less valuable. Therefore, the optimal value of

$$\lambda_{opt} = \lambda_{Min} = \frac{1}{Q_{lhv}} \leq \lambda \quad (45)$$

When the ECMS equivalence factor is large, the penalty for using electrical power is high and ECMS tends to charge the battery up to $SOC = SOC_H$. In this case, the vehicle operates in fuel only mode for most of the trip. When SOC is at the upper bond, the control action u is

$$\left.\begin{array}{c} x = SOC_H \\ P_D > 0 \end{array}\right\} \Longrightarrow u \in \{u_{eom}\} \cup \{u_{bom}\} \cup \{u_{hm}\} \quad (46)$$

where u_{eom} is the control action in engine only mode, u_{bom} is in battery only mode, and u_{hm} is in hybrid mode. Then, the Hamiltonian equations for these modes are shown below

$$H\left(u^*_{eom}\right) = \dot{m}_{fuel}\left(u^*_{eom}, P_D\right) + k\cdot\dot{Ah}_{eff}\left(x, u^*_{eom}\right) \quad (47)$$

$$H\left(u^*_{bom}\right) = \lambda P_{bat,C}\left(x, u^*_{bom}\right) + k\cdot\dot{Ah}_{eff}\left(x, u^*_{bom}\right) \quad (48)$$

$$H\left(u^*_{hm}\right) = \dot{m}_{fuel}\left(u^*_{hm}, P_D\right) + \lambda P_{bat,C}\left(x, u^*_{hm}\right) + k\cdot\dot{Ah}_{eff}\left(x, u^*_{hm}\right) \quad (49)$$

where u^* represents all the admissible control actions. When λ approaches infinity, then based on equation (35), the ECMS will never discharge the battery, because the cost of using the battery will always be higher than the cost of using fuel. Consequently, the vehicle will always be in engine only mode for any $P_D > 0$, and the SOC will stay at the upper limit since the battery is charged by Engine.

$$\left.\begin{array}{c} x = SOC_H \\ \lambda \gg \dfrac{1}{Q_{lhv}} \end{array}\right\} \Rightarrow \begin{cases} P_D > 0 : H\left(u_{eom}\right) < H(u^*_{bom}) \\ \quad and \\ P_D > 0 : H\left(u_{eom}\right) < H(u^*_{hm}) \end{cases} \quad (50)$$

Therefore, this large value of λ cannot be optimal for any drivecycle. An upper bound for λ^* can be obtained by decreasing of λ until use of the electric motors becomes feasible. For instance, the battery only mode and the hybrid mode will also have chance to be operated optimally.

$$\left.\begin{array}{c} x = SOC_H \\ \lambda = \lambda_{Max} \end{array}\right\} \Rightarrow \begin{cases} P_D > 0 : H\left(u_{eom}\right) > H(u^*_{bom}) \\ \quad or \\ P_D > 0 : H\left(u_{eom}\right) > H(u^*_{hm}) \end{cases} \quad (51)$$

The inequalities above shows that the upper bound of λ should allow battery discharging to be optimal. So $\lambda_{Max} = \min(\lambda_{Max1}, \lambda_{Max2})$, where λ_{Max1} is the upper bond λ value during battery only mode, λ_{Max2} is the upper bond λ value during hybrid mode.

When $\lambda = \lambda_{Max}$ and $SOC = SOC_H$, λ_{Max1} is calculated having battery only mode be more efficient than engine only mode (have a smaller Hamiltonian):

$$\begin{aligned} &H\left(u_{eom}\right) > H\left(u_{bom}\right) \\ &\dot{m}_{fuel}\left(u_{eom}, P_D\right) + k\cdot\dot{Ah}_{eff}\left(x, u_{eom}\right) \\ &\quad > \lambda^* P_{bat,C}\left(x, u_{bom}\right) + k\cdot\dot{Ah}_{eff}\left(x, u_{bom}\right) \end{aligned}$$

Therefore,

$$\lambda^* \leq \frac{\dot{m}_{fuel}\left(u_{eom}, P_D\right) + k\cdot\dot{Ah}_{eff}\left(x, u_{eom}\right) - k\cdot\dot{Ah}_{eff}\left(x, u_{bom}\right)}{P_{bat,C}\left(x, u_{bom}\right)} \quad (52)$$

In engine only mode (λ is very large), there will be few (only when the batteries are required to meet drivers demand) opportunities to use battery power. Therefore, the cost of the aging term $k\cdot\dot{Ah}_{eff}\left(x, u_{eom}\right) = 0$. In addition, when λ is relatively large, there is again limited opportunity to use the battery. So, $k\cdot\dot{Ah}_{eff}\left(x, u_{bom}\right)$ is approximately zero when λ is relatively large. Therefore, equation (52) is approximately

$$\lambda^* \leq \frac{\dot{m}_{fuel}\left(u_{eom}, P_D\right)}{P_{bat,C}\left(x, u_{bom}\right)} \quad (53)$$

Then

$$\lambda_{Max1} = \frac{\frac{P_D/\eta_{trs}(u^*_{eom})}{Q_{lhv}\eta_{eng}(u^*_{eom})}}{P_D/\eta_{trs}(u^*_{bom})/\eta_{em}\left(u^*_{bom}\right)\eta_{inv}\left(u^*_{bom}\right)\eta_{bat}\left(u^*_{bom}\right)}$$

$$\Rightarrow \lambda_{Max1} = \frac{\bar{\eta}_{em}\bar{\eta}_{inv}\bar{\eta}_{bat}}{Q_{lhv}\bar{\eta}_{eng}} \quad (54)$$

where η_{trs} is the transmission efficiency, η_{eng} is the engine efficiency, η_{em} is the e-machine efficiency, η_{inv} is the inverter efficiency, and η_{bat} is the battery efficiency. And $\bar{\eta}$ is the average efficiency of the powertrain component.

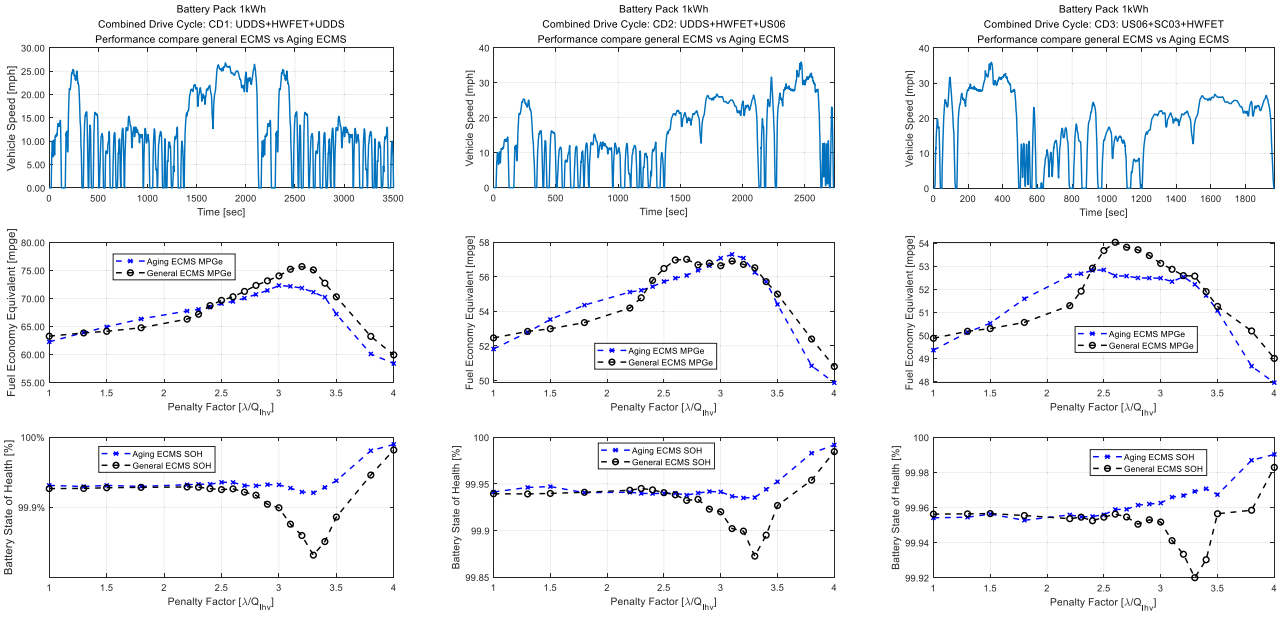

(a) (b) (c)

FIGURE 2. Combined drive cycles, vehicle speed, 1 kWh Fuel Economy Equivalent vs equivalence factors, 1 kWh Battery remaining State of Health vs equivalence factors. (a) CD1: UDDS+HWFET+UDDS; (b) CD2: UDDS+HWFET+US06; (c) CD3: US06+SC03+HWFET.

The second inequality in (51) requires that,

$$\lambda^* \leq \frac{\dot{m}_{fuel}\left(u_{eom}, P_D\right) - \dot{m}_{fuel}\left(u_{hm}, P_D\right)}{P_{bat,C}\left(x, u_{hm}\right)} \tag{55}$$

Therefor

$$\lambda_{Max2} = \frac{\frac{P_D/\eta_{trs}(u^*_{eom})}{Q_{lhv}\bar{\eta}_{eng}(u^*_{eom})} - \frac{P_D/\eta_{trs}(u^*_{eom}) - P_{em}(u^*_{hm})}{Q_{lhv}\bar{\eta}_{eng}(u^*_{hm})}}{\bar{\eta}_{en}\left(u^*_{hm}\right)\bar{\eta}_{inv}\left(u^*_{hm}\right)\bar{\eta}_{bat}\left(u^*_{hm}\right)}$$
$$\Rightarrow \lambda_{Max2} = \frac{\bar{\eta}_{em}\bar{\eta}_{inv}\bar{\eta}_{bat}}{Q_{lhv}\bar{\eta}_{eng}} \tag{56}$$

Therefore, the bounds of the equivalence factor for ECMS, given in Eq. (12), are still valid bounds for the equivalence factor in Aging ECMS.

IV. SIMULATION RESULTS

ECMS is a causal controller with a fixed equivalence factor since no information about the future driving conditions is being used to estimate λ [39]. Thus, the final SOC is not controllable. As a result, when comparing simulation results, the equivalent Miles per Gallon (MPGe) is employed. MPGe allows us to examine the total consumed energy and account for different final SOC values.

MPGe, as defined in [37] and used in [38], can be calculated by

$$MPGe = \frac{Distance}{Gallons_{fuel} + Gallons_{Equivalent}} \tag{57}$$

where $Gallons_{Equivalent}$ is gallons of gasoline equivalent to the consumed electric energy:

$$Gallons_{equivalent} = \frac{E_M}{E_G} \tag{58}$$

and E_M is total electric energy consumed, E_G is energy content per gallon of gasoline $32600 Wh/gallon$.

The Honda Civic IMA with the configuration shown in Fig.1 is used in this work. The detailed vehicle specifications are shown in Table 2. Three battery packs with 1 kWh, 2 kWh, and 4 kWh have been simulated to show the performance of the proposed ECMS with Aging consideration.

Three types of Combined Drive-cycles (CDs) have been tested for each simulation. These CDs were created by appending standard drive cycles in a sequence, as follows:

CD1: UDDS, HWFET, and UDDS
CD2: UDDS, HWFET, and US06
CD3: US06, SC03, and HWFET

These CDs simulate different types of daily driving behaviors, utilizing different percentages of highway, city, or country driving. Fig. 2 shows the vehicle speed for these three CDs. Fig. 2a includes the most of city driving with a total distance of 25.26 miles. Fig. 2b includes a balance between city and highway driving with a total distance of 25.77 miles. Fig. 2c includes the most highway driving with a total distance of 21.87 miles.

Fig. 2 also shows the MPGe and battery remaining state of health (SOH) across all equivalence factors within the bounds. When $\lambda = 1/Q_{lhv}$, the aging ECMS operates in electric only mode, the battery discharges at the beginning of

TABLE 2. Vehicle specification Honda Civic IMA parallel HEV.

Vehicle Components	Vehicle Specification
Configuration	Mild Parallel Hybrid
Vehicle mass	1279 Kg
Engine max torque	120 N·m @ 3500 rpm
E-machine max torque	62 N·m @ 2200 rpm
Battery energy	1.003 KW.hr 2.007 KW.hr 4.001 KW.hr
Battery cell capacity	3.5 Ah
Battery initial SOC	68.5%
Battery SOC range	50% to 70%
Battery OCV	3.8 V
Initial temperature	20 ℃

the drive cycle, and the SOC remains at the lower constraint SOC_L in the rest of the drive cycle. When $\lambda = 4/Q_{lhv}$, the aging ECMS operates in engine only mode, the battery charges at the beginning of the drive cycle, and the SOC remains at the upper constraint SOC_H. Therefore, the MPGe is lower at the values close to the equivalence factor bounds.

When λ/Q_{lhv} equals around 2.5 to 3.5, the aging ECMS operates in more hybrid mode, which causes more battery damage (fast charging-discharging events) and provides better fuel economy. As shown in Fig. 2, the aging ECMS algorithm significantly improves the battery SOH, especially at equivalence factors where the vehicle is operating in hybrid mode, for all three drive cycles. In addition, there is only a small fuel economy penalty all cases. Using 2 kWh and 4 kWh battery packs generated similar overall results.

Table 3 and Table 4 shows the optimal penalty factor for each combined drive cycle with 1 kWh, 2 kWh and 4 kWh battery packs. The MPGe and remaining SOH of both general ECMS and Aging ECMS are compared. The optimal equivalence factor which yields the best MPGe for both general ECMS and Aging ECMS are picked. As stated before, the MPGe has been picked to compare, because the causal ECMS and Aging ECMS algorithms cannot control the final SOC.

As shown in Table 4, aging ECMS saved 0.073% of battery aging in a 25.26 miles drive which traded off from 75.7 MPGe to 72.32 MPGe. Assume the price for gasoline is \$3 per gallon and the cost to replace the battery pack is \$207 per 1kWh battery [40] plus a \$200 replacement labor cost. Table 5 shows the economic performance comparison between general ECMS and aging ECMS. Fuel cost showed in Table 5 is calculated based on

$$Fuel\ Cost = \frac{CD\ Distance}{MPGe} \cdot FuelPrice \tag{59}$$

The battery cost is calculated from

$$Battery\ Cost = (1 - SOH) \cdot Battery\ Replacement \tag{60}$$

The total cost comparison is shown in Table 6.

TABLE 3. Optimal equivalence factor simulation results.

Battery pack	Drive Cycle	General ECMS $\lambda^* \cdot Q_{lhv}$	Aging ECMS $\lambda^* \cdot Q_{lhv}$
1 kWh	CD1	3.2	3
	CD2	2.7	3.1
	CD3	2.6	3.2
2 kWh	CD1	3.2	3.1
	CD2	2.8	3.2
	CD3	2.6	3.2
4 kWh	CD1	3.1	3.1
	CD2	2.8	3.1
	CD3	2.6	3.1

TABLE 4. Simulation results of the performance.

Battery pack	Drive Cycle	General ECMS		Aging ECMS	
		MPGe	*SOH*	*MPGe*	*SOH*
1 kWh	CD1	75.70	99.859%	72.32	99.932%
	CD2	57.01	99.932%	57.29	99.937%
	CD3	54.04	99.956%	52.54	99.967%
2 kWh	CD1	80.35	99.947%	76.56	99.966%
	CD2	59.26	99.969%	59.63	99.968%
	CD3	56.51	99.977%	54.88	99.981%
4 kWh	CD1	88.05	99.976%	85.21	99.980%
	CD2	63.57	99.983%	64.12	99.982%
	CD3	61.61	99.985%	59.67	99.986%

TABLE 5. Economic performance simulation results.

Battery pack	Drive Cycle	General ECMS [\$]		Aging ECMS [\$]	
		Fuel Cost	Battery Cost	Fuel Cost	Battery Cost
1 kWh	CD1	1.001	0.574	1.048	0.277
	CD2	1.356	0.277	1.349	0.256
	CD3	1.214	0.179	1.249	0.134
2 kWh	CD1	0.943	0.325	0.990	0.209
	CD2	1.305	0.190	1.296	0.196
	CD3	1.161	0.141	1.196	0.117
4 kWh	CD1	0.861	0.247	0.889	0.206
	CD2	1.216	0.175	1.206	0.185
	CD3	1.065	0.154	1.100	0.144

The smaller battery pack combined with more city driving saved the most total cost. This is because city driving requires the battery to be used more frequently for charging, discharging, regenerative braking and electric only operation. The smaller battery pack has smaller electric energy capacity compared to the energy capacity of the fuel tank. The smaller energy capacity requires more rapid changes in SOC, and quicker and more frequently charge discharge cycles. On the other hand, the total cost with the larger battery pack is less than with the smaller battery pack in the same drive cycle.

Battery cost in CD1 is larger than in other drive cycles in both general ECMS and aging ECMS. However, the

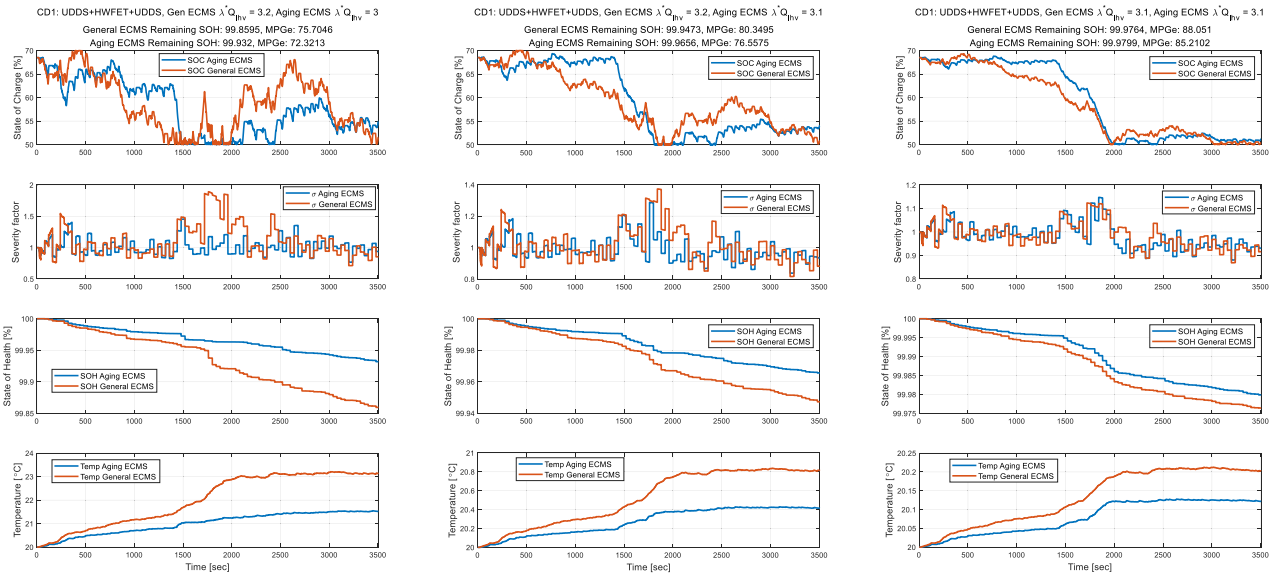

(a) (b) (c)

FIGURE 3. CD1 Performance, State of Charge, Severity Factor, State of Health and Battery temperature. (a) 1 kWh battery pack; (b) 2 kWh battery pack; (c) 4 kWh battery pack.

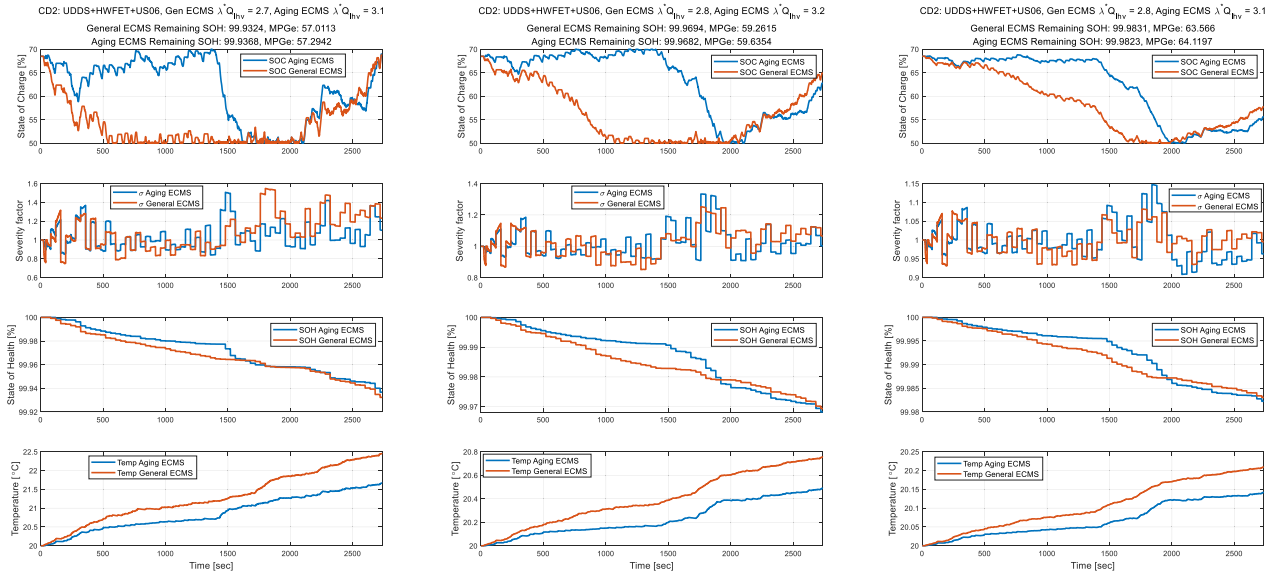

(a) (b) (c)

FIGURE 4. CD2 Performance, State of Charge, Severity Factor, State of Health and Battery temperature. (a) 1 kWh battery pack; (b) 2 kWh battery pack; (c) 4 kWh battery pack.

differences in CD1 of the battery cost are all smaller than other CDs in aging ECMS compare to general ECMS as shown in Table 5. CD2 has the largest cost of all battery packs, which is because the relatively longer distance of this drive cycle and less MPGe caused by the higher percentage of highway driving. CD3 is the drive cycle with the highest percentage of highway drives, which resulted the least MPGe in both general ECMS and aging ECMS. With 2 kWh and 4 kWh battery packs and the CD3 drive cycle, the cost of general ECMS is less than the aging ECMS. This is because in highway driving, less battery power is used, and the aging ECMS is not able to implement many control actions. However, the remaining SOH in CD3 is higher than other drive cycles as shown in Table 6.

Figs. 3, 4 and 5 shows the SOC variation, severity factor, SOH degradation, and battery temperature changes for 1 kWh, 2 kWh, 4 kWh battery packs in the three CDs. The optimal equivalence factor shown in Table 3 are picked and plotted.

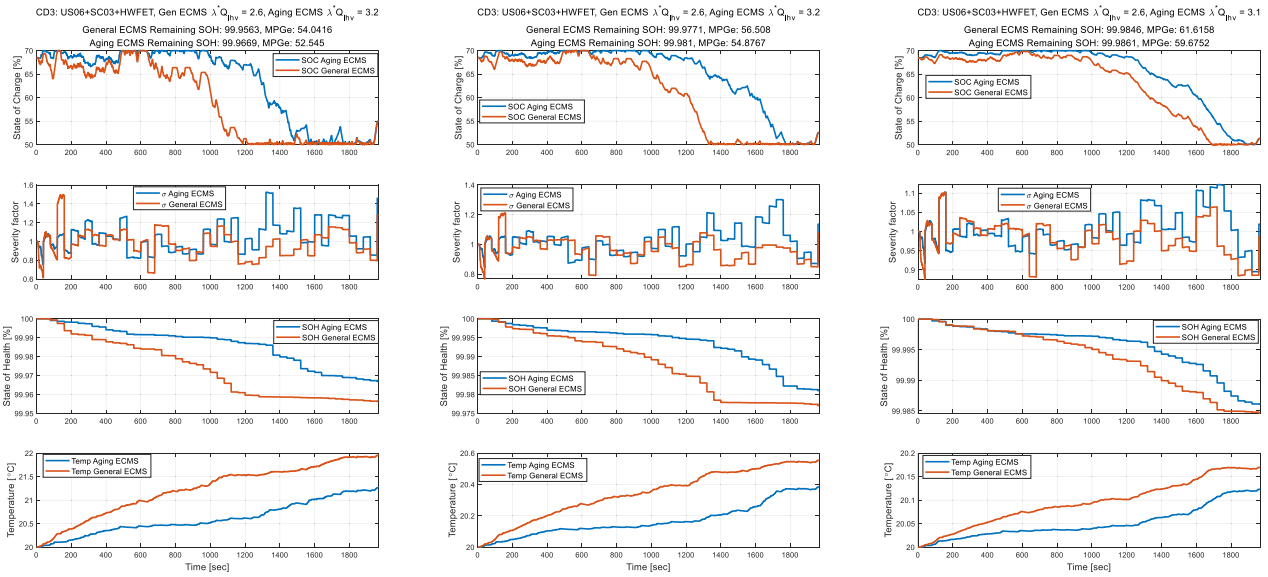

(a) (b) (c)

FIGURE 5. CD3 Performance, Performance, State of Charge, Severity Factor, State of Health and Battery temperature. (a) 1 kWh battery pack; (b) 2 kWh battery pack; (c) 4 kWh battery pack.

TABLE 6. Economic performance total cost.

Battery pack	Drive Cycle	General ECMS Total cost [$]	Aging ECMS total cost [$]	Percent saved
1 kWh	CD1	1.575	1.325	15.89%
	CD2	1.633	1.606	1.65%
	CD3	1.393	1.383	0.73%
2 kWh	CD1	1.269	1.198	5.52%
	CD2	1.495	1.493	0.13%
	CD3	1.302	1.312	-0.76%
4 kWh	CD1	1.107	1.095	1.12%
	CD2	1.391	1.391	0.01%
	CD3	1.219	1.243	-1.99%

It is obviously in Fig. 3 that the smaller battery pack has more rapid changes in State of Charge. In Fig. 3(a), aging ECMS takes the action to reduce the rapid charge-discharge cycles around 1800 seconds, and the severity factor and SOH plots shows that general ECMS produced critical damage during this time. In addition, Temperature plots also shows the temperature increases due to increased current. In Fig. 3(b) and (c), the amount of output current is the same, but the increase capacity of the battery leads to a smaller variation in SOC. The rapid increase in power demand is still the same, however, the requested power per battery cell has been reduced.

As shown in Fig. 4 and Fig.5, aging ECMS attempted to save battery life by reducing the ripples of the state of charge, which can also be seen in the temperature curve. All temperature plots show that aging ECMS generated less heat than general ECMS, which is because the total amount of discharges out from the battery is less compared to general ECMS. Similarly, SOH is decreased by the rapid discharge of the battery around 1400 seconds in CD2 and 1200 seconds in CD3. According to Fig. 2(b) and (c), this is caused by the rapid acceleration request from the driver. The battery has to provide a large amount of power to fully meet the demanded power from the driver.

V. CONCLUSION AND FUTURE WORKS

This paper introduces the aging ECMS control algorithm with a fixed equivalence factor. The Ah-throughput method has been used as the aging term in the ECMS cost function with regardless of the drive cycles. The aging coefficient has been found and correlated to the battery energy capacity the vehicle. This paper demonstrates that the equivalence factor in this algorithm is a constant. In addition, it is shown that with the new aging term added to ECMS, the bounds on the equivalence factor remain the same as for ECMS. The aging ECMS optimal controller presented does not require prediction or knowledge of future driving actions, which is causal controller for on-line applications.

From the simulation results, the performance of the aging ECMS algorithm significantly increased the battery life with little penalty to the fuel economy.

The bounds on the equivalence factor presented should also prove useful for designing new types of Adaptive-ECMS algorithms that incorporate battery aging considerations.

APPENDIX

In the vehicle model showed in Fig. 1, the total chemical power out of the battery pack $P_{bat,C}$ is defined:

$$P_{bat,C} = V_{bat,OC}\left(x\left(t\right)\right) I_{bat}\left(t\right)$$

where $V_{bat,OC}$ is the open-circuit voltage, I_{bat} is the battery pack current, $x(t)$ is the state of charge (SOC), Where Q_{bat} is the total battery capacity in $Amp \cdot sec$.

The electric machine used in this work is a Honda IMA 10kW electric motor. The electric machine and the inverter have been modeled as a single component based on a function of torque T_{em} and motor speed ω_{em}. Equation below given the function of the power request of electric machine P_{em}.

$$P_{em} = T_{em} \cdot \omega_{em} \cdot \eta_{em}(T_{em}, \omega_{em})$$

where η_{em} is the electric machine efficiency given by the steady-state map related to T_{em} and ω_{em} as shown in Fig. 6.

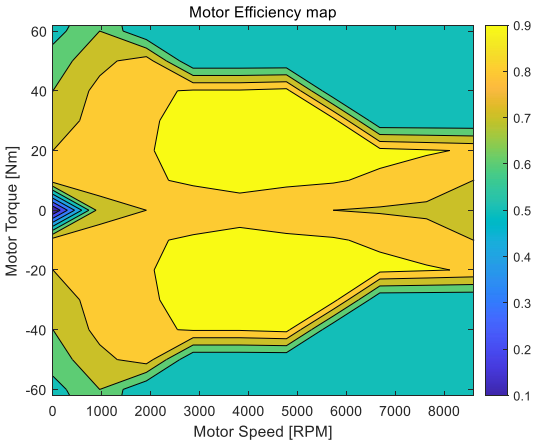

FIGURE 6. Motor efficiency map.

The transmission used in this brief is the Honda IMA 5 gear automated transmission. The transmission specifications for gear ratio r_{trs} are shown in Table 7 below.

TABLE 7. Honda IMA automatic transmission gear ratios.

1st gear	2nd gear	3rd gear	4th gear	5th gear	Final Drive
3.461	1.896	1.241	0.911	0.756	5.77

The final drive efficiency is set to 0.98, and the transmission gear shifting efficiency is set to 0.95.

The transmission shifting logic is based on the control action determined by the optimization strategy as well as the engine clutch control logic. When driver demanded power P_D is received, the ECMS calculates all the possible range of control actions, then based on the possible control actions, the consumed power has been calculated. Different transmission gear ratio is included in the options for consumed power. The ECMS then determine if the options of control actions are admissible, and calculates the cost of all the admissible controls, then choose the least cost control action option for vehicle's next step operation. Therefore, the transmission control is completed within the control actions selection by the ECMS as well as the clutch control.

The engine used in this brief is the Honda IMA 60 kW 4 cylinders engine. The engine output power P_{eng} is calculated from the power contained in fuel P_{fuel} which is given by equation below, and the engine efficiency map as shown in Fig. 7.

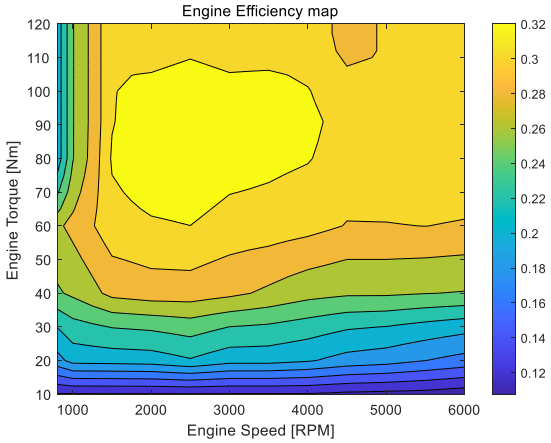

FIGURE 7. Engine efficiency map.

The fuel flow rate is given by a steady state map as shown in Fig. 8, which is a function of engine torque T_{eng} and engine speed ω_{eng}.

$$P_{eng} = \eta_{eng} \cdot P_{fuel} = \eta_{eng} \cdot Q_{lhv} \cdot \dot{m}_{fuel}(T_{eng}, \omega_{eng})$$

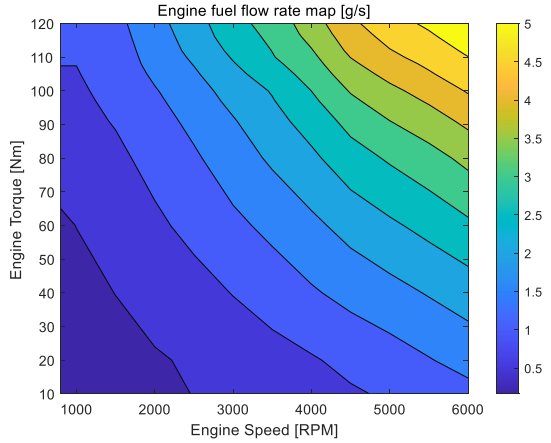

FIGURE 8. Engine fuel flow rate map.

where η_{eng} if the engine efficiency, P_{fuel} is the power contained in fuel with respect to the fuel flow rate $\dot{m}_{fuel}$. T_{eng} is the engine torque, and ω_{eng} is the engine speed in RPM.

REFERENCES

[1] A. Sciarretta and L. Guzzella, "Control of hybrid electric vehicles," *IEEE Control Syst.*, vol. 27, no. 2, pp. 60–70, Apr. 2007.
[2] S. Zhang, X. Hu, S. Xie, Z. Song, L. Hu, and C. Hou, "Adaptively coordinated optimization of battery aging and energy management in plug-in hybrid electric buses," *Appl. Energy*, vol. 256, Dec. 2019, Art. no. 113891.
[3] R. Du, X. Hu, S. Xie, L. Hu, Z. Zhang, and X. Lin, "Battery aging- and temperature-aware predictive energy management for hybrid electric vehicles," *J. Power Sources*, vol. 473, Oct. 2020, Art. no. 228568.

[4] S. Xie, X. Hu, Q. Zhang, X. Lin, B. Mu, and H. Ji, "Aging-aware co-optimization of battery size, depth of discharge, and energy management for plug-in hybrid electric vehicles," *J. Power Sources*, vol. 450, Feb. 2020, Art. no. 227638.

[5] Y. Bai, H. He, J. Li, S. Li, Y.-X. Wang, and Q. Yang, "Battery anti-aging control for a plug-in hybrid electric vehicle with a hierarchical optimization energy management strategy," *J. Cleaner Prod.*, vol. 237, Nov. 2019, Art. no. 117841.

[6] X. Hu, C. M. Martinez, and Y. Yang, "Charging, power management, and battery degradation mitigation in plug-in hybrid electric vehicles: A unified cost-optimal approach," *Mech. Syst. Signal Process.*, vol. 87, pp. 4–16, Mar. 2017.

[7] L. Tang and G. Rizzoni, "Energy management Strategy Including Battery Life Optimization for a HEV with a CVT," in *Proc. IEEE Transp. Electrific. Conf. Expo, Asia–Pacific (ITEC)*, Busan, South Korea, Jun. 2016, pp. 549–554.

[8] J. Wu, X. Wang, L. Li, C. Qin, and Y. Du, "Hierarchical control strategy with battery aging consideration for hybrid electric vehicle regenerative braking control," *Energy*, vol. 145, pp. 301–312, Feb. 2018.

[9] Y. Cai, M. G. Ouyang, and F. Yang, "Impact of power split configurations on fuel consumption and battery degradation in plug-in hybrid electric city buses," *Appl. Energy*, vol. 188, pp. 257–269, Feb. 2017.

[10] T. Hofman, M. Steinbuch, and R. M. Van Druten, "Rule-based energy management strategies for hybrid vehicles," *Int. J. Electr. Hybrid Vehicles*, vol. 1, no. 1, pp. 71–94, 2007.

[11] A. Rezaei, J. B. Burl, and B. Zhou, "Estimation of the ECMS equivalent factor bounds for hybrid electric vehicles," *IEEE Trans. Control Syst. Technol.*, vol. 26, no. 6, pp. 2198–2205, Nov. 2018, doi: 10.1109/TCST.2017.2740836.

[12] A. Rezaei, J. B. Burl, A. Solouk, B. Zhou, M. Rezaei, and M. Shahbakhti, "Catch energy saving opportunity (CESO), an instantaneous optimal energy management strategy for series hybrid electric vehicles," *Appl. Energy*, vol. 208, pp. 655–665, Dec. 2017.

[13] A. Rezaei and J. B. Burl, "Effects of time horizon on model predictive control for hybrid electric vehicles," *IFAC-PapersOnLine*, vol. 48, no. 15, pp. 252–256, 2015.

[14] D. E. Kirk, *Optimal Control Theory and Introduction*. Englewod Cliffs, NJ, USA: Prentice-Hall, 2004.

[15] N. Kim and A. P. Rousseau, "Comparison between rule-based and instantaneous optimization for a single-mode, power-split HEV," SAE Tech. Paper 2011-0873, 2011, doi: 10.4271/2011-01-0873.

[16] P. Pisu and G. Rizzoni, "A comparative study of supervisory control strategies for hybrid electric vehicles," *IEEE Trans. Control Syst. Technol.*, vol. 15, no. 3, pp. 506–518, May 2007.

[17] A. Rezaei and J. B. Burl, "Prediction of vehicle velocity for model predictive control," *IFAC-PapersOnLine*, vol. 48, no. 15, pp. 257–262, 2015.

[18] S. Onori and L. Tribioli, "Adaptive Pontryagin's minimum principle supervisory controller design for the plug-in hybrid GM Chevrolet Volt," *Appl. Energy*, vol. 147, pp. 34–224, Jun. 2015.

[19] C. Musardo, G. Rizzoni, and B. Staccia, "A-ECMS: An adaptive algorithm for hybrid electric vehicle energy management," in *Proc. 44th IEEE Conf. Decis. Control*, Seville, Spain, Jan. 2005, pp. 23–1816.

[20] A. Chasse, A. Sciarretta, and J. Chauvin, "Online optimal control of a parallel hybrid with costate adaptation rule," *IFAC Proc. Volumes*, vol. 43, no. 7, pp. 99–104, Jul. 2010.

[21] A. Chasse, G. Hafidi, P. Pognant-Gros, and A. Sciarretta, "Supervisory control of hybrid powertrains: An experimental benchmark of offline optimization and online energy management," *IFAC Proc. Volumes*, vol. 42, no. 26, pp. 109–117, 2009.

[22] M. S. H. Lipu, M. A. Hannan, A. Hussain, M. M. Hoque, P. J. Ker, M. H. M. Saad, and A. Ayob, "A review of state of health and remaining useful life estimation methods for lithium-ion battery in electric vehicles: Challenges and recommendations," *J. Cleaner Prod.*, vol. 205, pp. 115–133, Dec. 2018.

[23] J. Wang, P. Liu, J. Hicks-Garner, E. Sherman, S. Soukiazian, M. Verbrugge, H. Tataria, J. Musser, and P. Finamore, "Cycle-life model for graphite-LiFePO4 cells," *J. Power Sources*, vol. 196, no. 8, pp. 3942–3948, Apr. 2011.

[24] J. Vetter *et el.*, "Ageing mechanisms in lithium-ion batteries," *J. Power Sources*, vol. 147, nos. 1–2, pp. 269–281, 2005.

[25] H. Wenzl, I. Baring-Gould, R. Kaiser, B. Y. Liaw, P. Lundsager, J. Manwell, A. Ruddell, and V. Svoboda, "Life prediction of batteries for selecting the technically most suitable and cost effective battery," *J. Power Sources*, vol. 144, no. 2, pp. 373–384, Jun. 2005.

[26] L. Tang, G. Rizzoni, and S. Onori, "Energy management strategy for HEVs including battery life optimization," *IEEE Trans. Transport. Electrific.*, vol. 1, no. 3, pp. 211–222, Oct. 2015.

[27] Y.-H. Chiang, W.-Y. Sean, and J.-C. Ke, "Online estimation of internal resistance and open-circuit voltage of lithium-ion batteries in electric vehicles," *J. Power Sources*, vol. 196, no. 8, pp. 3921–3932, Apr. 2011.

[28] T. Feng, L. Yang, X. Zhao, H. Zhang, and J. Qiang, "Online identification of lithium-ion battery parameters based on an improved equivalent-circuit model and its implementation on battery state-of-power prediction," *J. Power Sources*, vol. 281, pp. 192–203, May 2015.

[29] Y. Ye, Y. Shi, N. Cai, J. Lee, and X. He, "Electro-thermal modeling and experimental validation for lithium ion battery," *J. Power Sources*, vol. 199, pp. 227–238, Feb. 2012.

[30] P. Rong and M. Pedram, "An analytical model for predicting the remaining battery capacity of lithium-ion batteries," *IEEE Trans. Very Large Scale Integr. (VLSI) Syst.*, vol. 14, no. 5, pp. 441–451, May 2006.

[31] A. Barre, F. Susard, M. Gerard, M. Montaru, and D. Riu, "Statistical method tools to analyze aging effects on Li-Ion battery performance," SAE Technical Paper 2013-1429, 2003.

[32] A. Barré, B. Deguilhem, S. Grolleau, M. Gérard, F. Suard, and D. Riu, "A review on lithium-ion battery ageing mechanisms and estimations for automotive applications," *J. Power Sources*, vol. 241, pp. 680–689, Nov. 2013.

[33] M. Debert, G. Colin, G. Bloch, and Y. Chamaillard, "An observer looks at the cell temperature in automotive battery packs," *Control Eng. Pract.*, vol. 21, no. 8, pp. 1035–1042, Aug. 2013.

[34] L. Serrao, S. Onori, A. Sciarretta, Y. Guezennec, and G. Rizzoni, "Optimal energy management of hybrid electric vehicles including battery aging," in *Proc. Amer. Control Conf.*, Jun./Jul. 2011, pp. 2125–2130.

[35] G. Suri and S. Onori, "A control-oriented cycle-life model for hybrid electric vehicle lithium-ion batteries," *Energy*, vol. 96, pp. 644–653, Feb. 2016.

[36] S. Onori, P. Spagnol, V. Marano, Y. Guezennec, and G. Rizzoni, "A new life estimation method for lithium-ion batteries in plug-in hybrid electric vehicles applications," *Int. J. Power Electron.*, vol. 4, no. 3, p. 302, 2012.

[37] P. Weissler. *Many Factors Figure in Fuel-Economy Calculation for Electric Vehicles*. Automotive Engineering Internal. Accessed: Aug. 2016. [Online]. Available: http://www.sae.org/mags/aei/6559/

[38] N. Higuchi, Y. Sunaga, M. Tanaka, and H. Shimada, "Development of a new two-motor plug-in hybrid system," *SAE Int. J. Alternative Powertrains*, vol. 2, no. 1, pp. 135–145, Apr. 2013.

[39] A. Rezaei, J. B. Burl, B. Zhou, and M. Rezaei, "A new real-time optimal energy management strategy for parallel hybrid electric vehicles," *IEEE Trans. Control Syst. Technol.*, vol. 27, no. 2, pp. 830–837, Mar. 2019, doi: 10.1109/TCST.2017.2775184.

[40] B. Halvorson. *Electric-Car Battery Prices Dropped 13% in 2019, Will Reach $100/KWH in 2023*. Green Car Rep. Accessed: Dec. 6, 2019. [Online]. Available: https://www.greencarreports.com/news/1126308_electric-car-battery-prices-dropped-13-in-2019-will-reach-100-kwh-in-2023

[41] S. Onori, L. Serrao, and G. Rizzoni, "Hybrid electric vehicles: Energy management strategies," in *Briefs Control, Automation and Robotics*. New York, NY, USA: Springer, 2016, chs. 4–7.

[42] N. Kim, S. Cha, and H. Peng, "Optimal control of hybrid electric vehicles based on Pontryagin's minimum principle," *IEEE Trans. Control Syst. Technol.*, vol. 19, no. 5, pp. 1279–1287, Sep. 2011.

[43] L. Guzzella and A. Sciarretta, *Vehicle propulsion Systems: Introduction to Modeling and Optimization*, 3rd ed. New York, NY, USA: Springer, 2013, ch. 7.

[44] B. Zhou, J. B. Burl, and A. Rezaei, "Effect of state of charge constraints on fuel economy and battery aging when using the equivalent consumption minimization strategy," SAE Tech. Paper 2018-01-1002, 2018, doi: 10.4271/2018-01-1002.

[45] B. Zhou, J. B. Burl, and A. Rezaei, "Effect of battery temperature on fuel economy and battery aging when using the equivalent consumption minimization strategy for hybrid electric vehicles," SAE Tech. Paper 2020-01-1188, 2018, doi: 10.4271/2020-01-1188.